

## Dynamics of Associative Polymers with High Density of Reversible Bonds

Shifeng Nian<sup>1,\*</sup>, Shalin Patil<sup>4,\*</sup>, Siteng Zhang,<sup>5</sup> Myoem Kim,<sup>1</sup> Quan Chen,<sup>6</sup> Mikhail Zhernenkov,<sup>7</sup>  
Ting Ge,<sup>5</sup> Shiwang Cheng<sup>4,‡</sup> and Li-Heng Cai (蔡历恒)<sup>1,2,3,†</sup>

<sup>1</sup>*Soft Biomatter Laboratory, Department of Materials Science and Engineering,  
University of Virginia, Charlottesville, Virginia 22904, USA*

<sup>2</sup>*Department of Chemical Engineering, University of Virginia, Charlottesville, Virginia 22904, USA*


<sup>3</sup>*Department of Biomedical Engineering, University of Virginia, Charlottesville, Virginia 22904, USA*

<sup>4</sup>*Department of Chemical Engineering and Materials Science, Michigan State University, East Lansing, Michigan 48824, USA*

<sup>5</sup>*Department of Chemistry and Biochemistry, University of South Carolina, Columbia, South Carolina 29208, USA*

<sup>6</sup>*State Key Lab Polymer Physics and Chemistry, Changchun Institute of Applied Chemistry,  
Renmin St. 5625, Changchun 130022, Jilin, People's Republic of China*

<sup>7</sup>*National Synchrotron Light Source-II, Brookhaven National Laboratory, Upton, New York 11973, USA*

 (Received 3 May 2022; revised 2 February 2023; accepted 19 April 2023; published 31 May 2023)

An associative polymer carries many stickers that can form reversible associations. For more than 30 years, the understanding has been that reversible associations change the shape of linear viscoelastic spectra by adding a rubbery plateau in the intermediate frequency range, at which associations have not yet relaxed and thus effectively act as crosslinks. Here, we design and synthesize new classes of unentangled associative polymers carrying unprecedentedly high fractions of stickers, up to eight per Kuhn segment, that can form strong pairwise hydrogen bonding of  $\sim 20k_B T$  without microphase separation. We experimentally show that reversible bonds significantly slow down the polymer dynamics but nearly do not change the shape of linear viscoelastic spectra. This behavior can be explained by a renormalized Rouse model that highlights an unexpected influence of reversible bonds on the structural relaxation of associative polymers.

DOI: [10.1103/PhysRevLett.130.228101](https://doi.org/10.1103/PhysRevLett.130.228101)

An associative polymer may carry many moieties that can form reversible bonds (Ref. [1] and therein). Unlike permanent covalent bonds, a reversible association can break and reform at laboratory timescales [2–9]. This process not only slows down polymer dynamics but also dissipates energy, enabling macroscopic properties inaccessible by conventional polymers. As a result, associative polymers provide solutions to some of the most pressing challenges in sustainability and health (Ref. [10] and therein). For example, associative polymers are widely used as viscosity modifiers for fuels [11], lubricants [12], and paints [13], to create tough self-healing polymers [14,15] and reprocessable supramolecular polymer networks [16–20], and to engineer biomaterials with prescribed dynamic mechanical properties critical to tissue engineering and regeneration [21,22]. Thus, understanding the effects of reversible interactions on the dynamics of associative polymers is of both technological and fundamental importance.

All existing understanding of associative polymers is built on a fundamental timescale—the lifetime of a reversible association  $\tau_s$ , which increases exponentially with the activation energy  $E_a$  [1,23–25]:

$$\tau_s = \tau_0 \exp\left(\frac{E_a}{k_B T}\right). \quad (1)$$

Here,  $k_B$  is the Boltzmann constant,  $T$  is the absolute temperature, and  $\tau_0$  the relaxation time of a Kuhn monomer in the absence of stickers. Equation (1) implies two widely accepted physical consequences about the dynamics of associative polymers. First, the structural relaxation time  $\tau_0$  is assumed to be independent of the concentration of stickers. Second, introducing associations changes the shape of the viscoelastic spectra by adding a rubbery plateau between the structural relaxation and the lifetime of the association, below which the associations have not yet relaxed and thus effectively act as crosslinks. Moreover, the width of the plateau,  $\tau_s/\tau_0$ , increases exponentially with the activation energy.

The activation energy,  $E_a$ , is defined as the strength of an association. For relatively simple pairwise associations such as hydrogen bonding, the activation energy has been assumed to be a constant determined by the bond strength. This is the foundational assumption for all existing theoretical models (Refs. [24,26–29] and therein) including ours [25]. Experimentally, the activation energy is measured through the change of polymer dynamics [23,30–32]. However, in *almost all* existing solvent-free experimental systems, the interaction between stickers often leads to nanoscale aggregations or even microphase separation; examples include clusters formed by hydrogen-bonding

groups at the two ends of a linear telechelic polymer [11,28,31,33–37] and  $\pi$ - $\pi$  stacking of quadruple hydrogen bonding formed by 2-ureido-4[1H]-pyrimidinone groups [38]. Because the nanoscale cluster is distinct from its surrounding environment, it creates both entropic and enthalpic barriers that prevent dissociation; this precludes a precise interpretation of experimentally measured activation energy. Alternatively, dynamic hydrogels cross-linked by reversible associations can be free of microphase separation [10]. However, hydrogels contain solvents that prevent probing the full linear viscoelastic spectra. As a result, it has yet to be rigorously tested the relation between the activation energy and the bond strength and the effects of reversible interactions on the dynamics of associative polymers.

In this Letter, we seek to experimentally answer two fundamental questions about associative polymers. First, what is the relation between the activation energy and the bond strength of a pairwise association? Second, would the reversible interactions affect the shape of linear viscoelastic spectra of associative polymers? We are interested in polymers with high concentrations of stickers close to and higher than one per Kuhn segment. Such high concentrations often occur in experimental systems, and sometimes are even required to create polymeric materials with optimized properties such as high stiffness and rapid self-healing ability [18,19,39]. Yet little is understood about the dynamics of associative polymers with high density of reversible bonds.

We design model associative polymers using amide groups as stickers, which form pairwise double hydrogen bonding without microphase separation at high concentrations of stickers [39]. We copolymerize two monomers, hexyl acrylate (HA) and 5-acetamido-1-pentyl acrylate (AAPA), to create an associative polymer,  $(HA_{1-\lambda}AAPA_{\lambda})_n$ , in which  $n$  is the degree of polymerization (DP) and  $\lambda$  is the molar fraction of the sticky monomer AAPA [Figs. 1(a) and 1(b)]. Two sticky monomers can form an amide-amide double hydrogen bond that crosslinks the polymers to form a transient network [Figs. 1(c) and 1(d)]. Compared to the spacer monomer HA, AAPA is essentially the same except that it carries an amide group at one of its ends [Fig. 1(a)]. Thus, it is reasonable to assume that the Kuhn length  $b$  of a reversible polymer does not change with  $\lambda$ . Each Kuhn segment consists of on average 8.7 chemical repeating units and that  $b = 22 \text{ \AA}$  (Sec. 1 of the Supplemental Material [40]). The calculated entanglement modulus of PHA,  $G_e = 110 \text{ kPa}$ , agrees well with experiments (dashed line in Fig. S3 [40]). These results provide the basic polymer physics parameters of associative polymers.

We develop a procedure to synthesize associative polymers with a fixed DP  $\sim 250$  but various  $\lambda$  of 0, 0.084, 0.25, 0.52, 0.75, and 1.0 (Fig. S1, Tables S1 and S2, Secs. 1–3 of the Supplemental Material [40]); these correspond to on average 0, 0.7, 2, 4, 6, and 8 stickers per Kuhn segment.

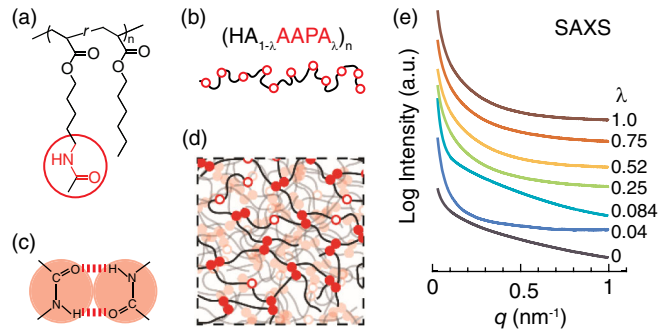


FIG. 1. Molecular design and structure of associative polymers. (a) An associative polymer is synthesized by copolymerizing HA and AAPA monomers. (b) Open circles: unpaired amide groups (“open” stickers);  $\lambda$ : fraction of stickers;  $n$ : degree of polymerization (DP). (c) Two amide groups form a pairwise hydrogen bond of strength  $\epsilon_b \approx 20k_B T$ . Shaded solid circles: “closed” stickers. (d) A schematic of an associative polymer network. (e) SAXS profiles of all unentangled associative polymers.

Moreover, the polymer MW 39 kDa is below the critical value  $M_c \approx 46 \text{ kDa}$ , such that the effects of entanglements are negligible. All polymers form homogeneous, amorphous liquids without nanoscale clusters, as evidenced by the absence of characteristic peaks from small-angle x-ray scattering (SAXS) measurements [Figs. 1(e) and S2] [57]. Importantly, the amide-amide bond is relatively strong,  $\epsilon_b \approx 20k_B T$  [58], such that its effects on polymer dynamics, if any, can be experimentally revealed.

The addition of stickers dramatically increases the glass transition temperature  $T_g$  of associative polymers, as shown by differential scanning calorimetry measurements in Fig. S4 [40]. As  $\lambda$  increases from 0 to 1,  $T_g$  increases from  $-62.9 \text{ }^\circ\text{C}$  to  $-14.5 \text{ }^\circ\text{C}$  (circles, Fig. 2). Yet, increasing the polymer MW from 39 to 157 kDa does not alter  $T_g$  (squares, Fig. 2). Interestingly, the measured  $T_g$  is higher than that predicted by the Fox relation [59]:  $1/T_g^\lambda = \sum_i f_i/T_g^i$ , where  $T_g^i$  is the  $T_g$  of homopolymer  $i$ , and  $f_i$  is the mass fraction of monomer units  $i$  in the copolymer (dash-dotted line in Fig. 2). Moreover, the change of  $T_g$  exhibits a nonlinear dependence on  $\lambda$ , contrasting recent theoretical prediction for a linear dependence in  $T_g$  shift for associative polymers with nanoscale aggregations [28] (inset, Fig. 2). Further,  $^1\text{H-NMR}$  measurements indicate a negligible amount of moisture nor residue solvents in associative polymers (Sec. 1.8 of the Supplemental Material [40]). These differences in  $T_g$  between our experiments and recent theories highlight the unique glass transition behavior of homogeneous associative polymers with high sticker density (Sec. 1.3 of the Supplemental Material [40]). Importantly, the dramatic increase in  $T_g$  implies that reversible interactions enhance monomeric friction to slow down polymer dynamics.

To further explore polymer dynamics, we quantify the linear viscoelasticity of polymers (Sec. 2 of the Supplemental

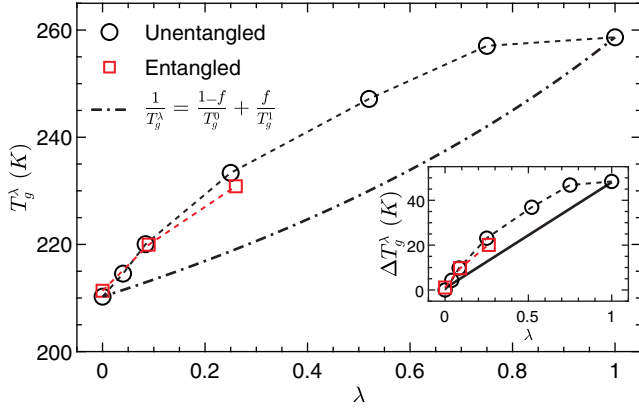


FIG. 2. The glass transition temperature  $T_g^\lambda$  of associative polymers with  $\lambda$  stickers. Dash-dotted line: Fox relation for  $T_g^\lambda$  using the weight fraction  $f$  of stickers as the variable. Circles: unentangled polymers with DP $\sim$ 250; squares: entangled polymers with DP $\sim$ 1000 (Fig. S4 [40]). Dashed line: guidance for the eye. Inset:  $\Delta T_g^\lambda \equiv T_g^\lambda - T_g^0$  vs  $\lambda$ . Solid line: theoretical prediction for telechelic associative polymers [28].

Material [40]) and use time-temperature superposition [60] to construct master curves for the dependencies of storage  $G'(\omega)$  and loss  $G''(\omega)$  moduli on oscillatory shear frequency  $\omega$ . Remarkably, the dynamics of the polymer with on average 0.7 stickers per Kuhn segment ( $\lambda = 0.084$ ) is nearly identical to that of the reference polymer without stickers (Fig. 3). By contrast, existing theories predict that, for a bonding strength  $\epsilon_b \approx 20 k_B T$ , the terminal relaxation should be slowed by at least  $\tau_s/\tau_0 \sim \exp(\epsilon_b/k_B T) \sim 10^8$  times

[Eq. (1)]. Such a dramatic discrepancy demonstrates an unexpected weak influence of strong reversible interactions on the linear viscoelasticity of associative polymers without microphase separation.

Further increasing sticker fraction significantly shifts the master curves to lower frequencies (Fig. 3). Yet, the master curves can be horizontally shifted to nearly perfect overlap with each other in the intermediate and low frequency regions (Figs. S5–S7). These results show that reversible associations slow down polymer dynamics but almost do not change the shape of the viscoelastic spectra. This behavior is in striking contrast to that predicted by the classic sticky-Rouse model for unentangled associative polymers: reversible associations change the shape of linear viscoelastic spectra by adding a rubbery plateau in the intermediate frequency range, at which associations have not yet relaxed and thus effectively act as crosslinks [31,33,35,62–65].

To explain our remarkable observations, we propose a *renormalized* Rouse model to account two unique features of our associative polymers: (i) the fractions of stickers are high with values no less than one per Kuhn segment; (ii) there is no microphase separation in the melt. Thus, although a reversible polymer is a random copolymer consisting of spacer and sticky monomers, there is no chemical and physical inhomogeneity at length scales no smaller than Kuhn segment, the elementary unit of polymer physics models. We therefore treat the reversible polymer as a homopolymer consisting of *renormalized* Kuhn segments with a relaxation time  $\tau_{s0}$ . The Rouse relaxation modulus for polymers with sticker fraction  $\lambda$  is

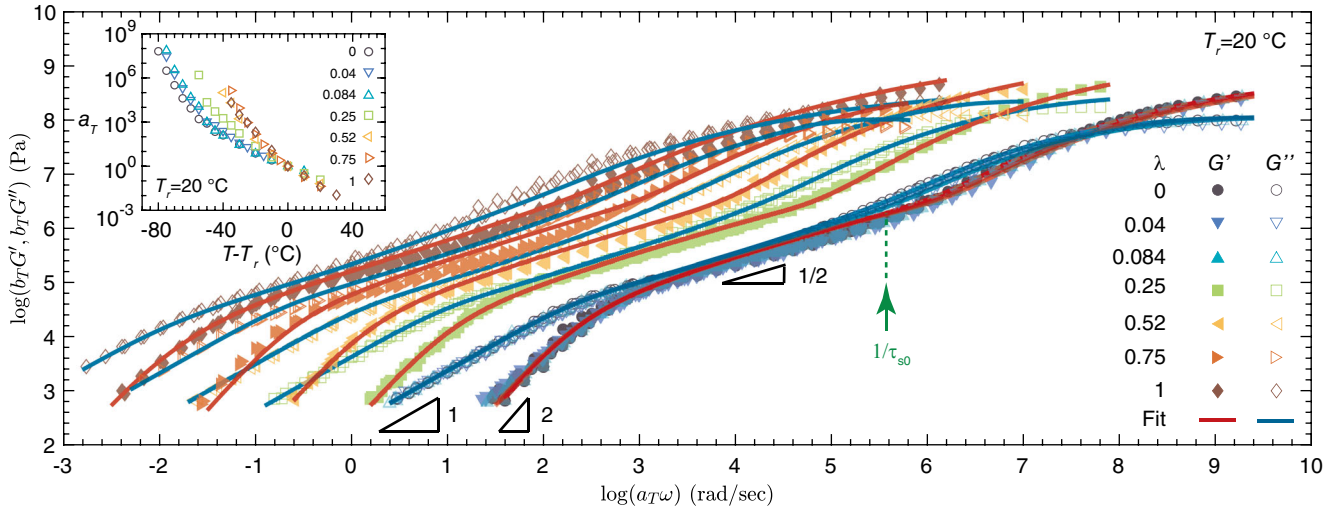


FIG. 3. Linear viscoelasticity of unentangled associative polymers. Master curves of storage ( $G'$ ) and loss ( $G''$ ) moduli as a function of angular frequency  $\omega$  at a reference temperature  $T_r = 20^\circ\text{C}$ . Solid lines represent the fit of the sum of *renormalized* Rouse model for low-frequency behavior,  $G_{rR}(t)$  [Eq. (2)], and Kohlrausch-Williams-Watts (KWW) model [61],  $G_g(t) = G_g(0) \exp[-(t/\tau_{KWW})^\beta]$ , for high-frequency glassy dynamics:  $G(t) = G_{rR}(t) + G_g(t)$ .  $G_g(0)$ : glassy modulus at  $t \rightarrow 0$ ;  $\tau_{KWW}$ : characteristic time of glass relaxation.  $\beta$  describes the distribution of glass relaxation modes: The lower the value of  $\beta$ , the broader the mode distribution (Sec. 1.6 of the Supplemental Material [40]); fitting parameters are listed in Table S1. The modulus shift factors  $b_T = \rho T / \rho_r T_r$ , where  $\rho_r$  is the polymer density at  $T_r$ , and  $T$  is the absolute temperature at which measurements are performed. Inset: timescale shift factors  $a_T$ .

$$G_{rR}(t, \lambda) = \sum_i N_{A_i} k_B T \frac{\rho w_{i,\lambda}}{M_{i,\lambda}} \sum_{q=1}^{N_{i,\lambda}} \exp\left(-\frac{t q^2}{\tau_{s0} N_{i,\lambda}^2}\right), \quad (2)$$

in which  $w_{i,\lambda}$ ,  $M_{i,\lambda}$ , and  $N_{i,\lambda} = M_{i,\lambda}/M_0(\lambda)$  are, respectively, the weight fraction, MW, and the number of Kuhn monomers of the  $i$ th polymer with sticker fraction  $\lambda$ . Here  $M_0(\lambda) = n_k[m_{\text{HA}}(1-\lambda) + m_{\text{AAPA}}\lambda]$  is the mass of a Kuhn monomer with sticker fraction  $\lambda$ , in which  $m_{\text{HA}} = 156$  Da,  $m_{\text{AAPA}} = 199$  Da, and the  $n_k = 8.7$  is the number of chemical monomers per Kuhn segment.

We emphasize that  $\tau_{s0}$  cannot be viewed as the renormalized lifetime of a sticker in the classic sticky-Rouse model [25,37]. In this model, the renormalized lifetime is defined as the average time for a closed sticker to dissociate from a bond to form a new bond with a new open sticker. Thus, it becomes easier for an open sticker to find a new partner at higher concentrations of stickers. And the sticky-Rouse model predicts that the renormalized lifetime decreases with the sticker concentration [25]. By contrast, for our associative polymers, each renormalized Kuhn segment is an effective sticker, and the concentration of effective stickers is always a constant one. Thus,  $\tau_{s0}$  can be viewed as the basic monomeric relaxation time of the renormalized polymers.

We quantify  $\tau_{s0}$  by using Eq. (2) to fit the low  $\omega$  relaxation behavior of the measured moduli [30]. In Eq. (2), the MW distribution  $w_{i,\lambda}$  is directly determined from size exclusion chromatography (Sec. 2 of the Supplemental Material [40]), and the basic polymer physics parameters are predetermined from synthesis. Thus, all input parameters are given by experiments except  $\tau_{s0}$ . Using  $\tau_{s0}$  as the only adjustable parameter, we obtain nearly perfect fit to experiments [lines in Fig. 3(b)]. This one-parameter fitting allows precise quantification of  $\tau_{s0}(\lambda, T_r)$ , as listed in Table S1 [40].

Interestingly, at reference temperature  $T_r = 20^\circ\text{C}$  the segmental relaxation time increases nearly exponentially with  $\lambda$ :

$$\tau_{s0}(\lambda, T_r) = \tau_{s0}(0, T_r) \exp(\alpha_{T_r} \lambda), \quad (3)$$

in which  $\tau_{s0}(0, T_r) = 3.7 \times 10^{-7}$  sec is the relaxation time of a PHA Kuhn monomer without reversible interactions, and  $\alpha_{T_r}$  is a fitting parameter of  $8.9 \pm 1.2$  [dashed line to squares in Fig. 4(a)]. Accounting for the correction of  $\tau_{s0}$  due to the slight increase in monomer mass with  $\lambda$  results in a negligible difference [solid line to circles in Fig. 4(a)]. Expression (3) indicates that at room temperature the apparent activation energy increases linearly with the concentration of stickers,  $E_a/k_B T_r = \alpha_{T_r} \lambda$ . This behavior contrasts the widely accepted understanding that the activation energy is independent of sticker concentration [24–29]. Moreover, as the reference temperature

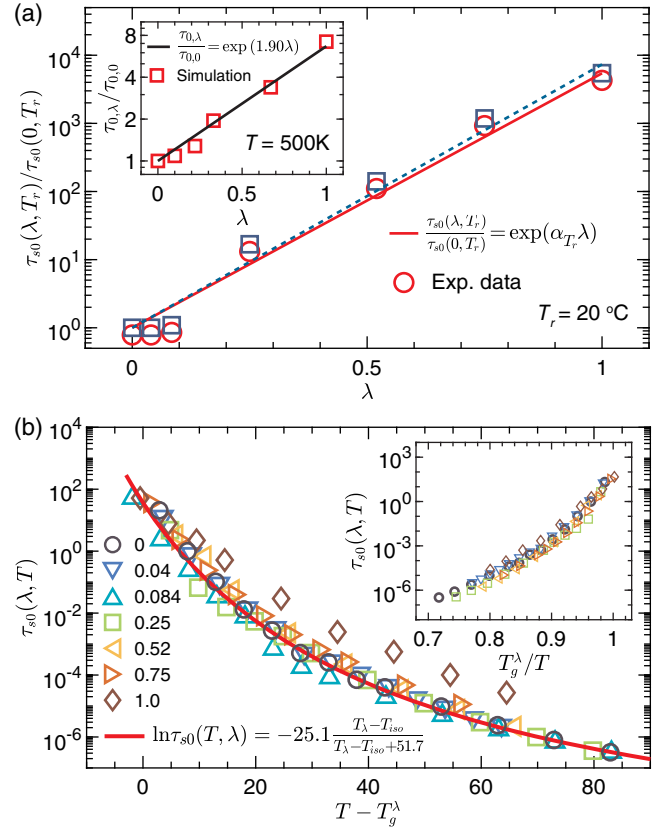


FIG. 4. Structural relaxation of unentangled associative polymers. (a) Relaxation time of a renormalized Kuhn monomer,  $\tau_{s0}$ , at  $T_r = 20^\circ\text{C}$ . Lines are the best fit to experiments using Eq. (3). Dashed line is for data (squares) using the relaxation of a pure PHA monomer as  $\tau_{s0}(0, T_r)$ , and the fitting parameter  $\alpha_{T_r} = 8.9 \pm 1.2$  [Eq. (3)]. Solid line is for data (circles) with the correction of  $\tau_{s0}$  due to the slight increase in monomer mass with  $\lambda$ , and  $\alpha_{T_r} = 8.6 \pm 1.2$ . Inset: Diffusion time  $\tau_{0,\lambda}$  of a 9-mer molecule vs  $\lambda$  in the atomistic simulations at  $T = 500$  K. (b)  $\tau_{s0}(\lambda, T)$  at various temperatures and  $\lambda$  vs  $T - T_g^\lambda$ . Solid line: the best using Eq. (4). Inset:  $\tau_{s0}$  vs reduced temperature  $T_g^\lambda/T$ .

decreases,  $\alpha_{T_r}$  increases but similar linear dependence persists (Fig. S8 [40]). The experimentally observed linear behavior can be qualitatively captured by atomistic simulation for melts of pure Kuhn monomers at a high temperature 500 K, which reveals that the relaxation time of a Kuhn monomer increases exponentially with the fraction of stickers [inset, Fig. 4(a); Sec. 1.7 of the Supplemental Material [40]]. These results show that despite a linear dependence of the apparent activation energy on the fraction of stickers, there is no direct connection between the strength of a pairwise bond and the absolute value of the activation energy. Importantly, our results indicate that the apparent activation energy depends on temperature.

To explore the dependence of segmental relaxation time on temperature, we construct the master curves at various reference temperatures, and use the same procedure to

determine  $\tau_{s0}(\lambda, T)$ . Remarkably, plotting  $\tau_{s0}(\lambda, T)$  against  $T_g^\lambda/T$  collapses almost all monomeric relaxation times to a master curve [inset, Fig. 4(b)]. Similarly, a master curve is obtained by plotting  $\tau_{s0}(\lambda, T)$  against the distance from glass transition,  $T - T_g^\lambda$  [symbols in Fig. 4(b)]. Moreover, the master curves can be described by a non-Arrhenius, Williams-Landel-Ferry like dependence on temperature [solid line in Fig. 4(b)]:

$$\ln \tau_{s0}(T, \lambda) = -25.1 \frac{T_\lambda - T_{\text{iso}}}{T_\lambda - T_{\text{iso}} + 51.7}, \quad (4)$$

in which  $T_\lambda \equiv T - T_g^\lambda$ , and  $T_{\text{iso}} = 6.5^\circ\text{C}$  is the isofrictional temperature. Here, the fitting parameters  $25.1 \pm 1.1$  and  $(51.7 \pm 4.1)$  K are valid to our associative polymers but not necessarily to other polymers. The first parameter is related to the free volume at  $T_r$ , whereas the latter is related to the Vogel temperature at which the free volume is zero, which is about 50 K below the glass transition [60].

Equation (4) indicates that, for any fixed sticker fraction, the temperature dependence of the ratio between the lifetime of a renormalized Kuhn segment to that of a Kuhn segment without stickers,  $[d/d(1/T)] \ln[\tau_{s0}(T, \lambda \neq 0)/\tau_{s0}(T, 0)]$ , is not a constant. Thus, for a given  $\lambda$ , a constant apparent activation energy cannot be obtained across the explored temperatures. This behavior is consistent with the temperature dependence of  $\alpha_{T_r}$  [Eq. (3)], but is fundamentally different from the classic sticky-Rouse model that has a constant activation energy at all temperatures [Eq. (1)]. Understanding the molecular origin of reversible interactions on structural relaxation is beyond the scope of this Letter and will be the subject of future explorations. Nevertheless, our results show that the *renormalized* Rouse model provides a universal description of the dynamics of associative polymers with high densities of reversible bonds: Reversible interactions slow down the polymer dynamics by decreasing the elementary timescale associated with structural relaxation without changing the shape of linear viscoelastic spectra of polymers.

In summary, we have developed unentangled associative polymers carrying unprecedented high concentrations of stickers that can form pairwise interactions without microphase separation. The reversible interactions significantly slow down the polymer dynamics but nearly do not change the shape of linear viscoelastic spectra. Our experimental observation can be well described by a *renormalized* Rouse model, in which a reversible polymer is treated as a homopolymer consisting of *renormalized* Kuhn monomers. The segmental relaxation time  $\tau_{s0}(\lambda, T)$  depends on both the concentration of stickers and temperature. Remarkably, at a given temperature,  $\tau_{s0}(\lambda, T)$  increases exponentially with the concentration of stickers. Moreover, introducing stickers increases the polymer glass transition temperature. Although the increase does not follow the Fox relation, it is

in line with the slowdown of polymer dynamics, which exhibit a universal yet non-Arrhenius dependence of structural relaxation time on the distance from glass transition temperature.

At a relatively low fraction of stickers, 0.3 per Kuhn segment ( $\lambda = 0.04$ ), the polymer exhibits no microphase separation [Fig. 1(e)] and a negligible slowdown in polymer dynamics (Fig. S5). Together with the data on high sticker concentrations, this behavior suggests that the absence of microphase separation is critical to the observed unconventional linear viscoelasticity of associative polymers. Further, it implies that the concept of renormalization may be extended to sticker fractions less than one per Kuhn segment. However, it has yet to be determined whether the renormalized Rouse model holds at very low sticker fractions, as there may be a critical sticker fraction below which the dynamics behaves like classical telechelic associative polymers [28]. Interestingly, the width of the glass transition zone increases with sticker density (Fig. 3, Table S1, and Sec. 1.6 of the Supplemental Material [40]). Moreover, at the maximum sticker concentration ( $\lambda = 1$ ), the shift factors deviate from the master curve [diamonds, Fig. 4(b)]. We speculate that reversible interactions promote local alignment of Kuhn segments to facilitate their cooperative motion; this would increase the number of relaxation modes and thus broaden the glass transition zone.

Nevertheless, our findings reveal an unexpected influence of reversible interactions on the structural relaxation rather than the viscoelastic spectra of associative polymers. Thus, our associative polymers provide a system that allows for investigating separately the effects of reversible interactions on chain relaxation and glassy dynamics; this may offer opportunities to improve the understanding of the challenging physics of glass transition of polymers [66]. Perhaps more importantly, our discoveries show that the fraction of stickers, in addition to the conventionally thought sticker-sticker binding energy, is another dominant parameter controlling the dynamics of associative polymers without microphase separation, and thus represent a paradigm shift in the development of supramolecular materials [18,21].

L. H. C. acknowledges support from NSF (CAREER DMR-1944625), ACS Petroleum Research Fund (PRF) (6132047-DNI), Virginia Commonwealth Health Research Grant, and Juvenile Diabetes Research Foundation. L. H. C. conceived and oversaw the study. L. H. C., S. N., S. C., and S. P. designed the research. S. N. synthesized and characterized the polymers and M. K. helped with the synthesis. S. P. performed DSC and rheological measurements under S. C.'s supervision. S. Z. performed atomistic simulation under T. G.'s supervision. Q. C. provided initial code for fitting the linear viscoelasticity data. M. Z. helped with SAXS measurements. L. H. C. and S. C. analyzed the

data. L. H. C. developed theoretical models and wrote the paper. All authors reviewed and commented on the paper. L. H. C. and S. N. have filed a patent for the synthesis and use of reversible polymers (U.S. Provisional Patent No. 63/193,344).

\*These authors contributed equally to this work.

†Corresponding author.

liheng.cai@virginia.edu

‡chengsh9@msu.edu

- [1] Z. Zhang, Q. Chen, and R. H. Colby, Dynamics of associative polymers, *Soft Matter* **14**, 2961 (2018).
- [2] L. Leibler, M. Rubinstein, and R. H. Colby, Dynamics of reversible networks, *Macromolecules* **24**, 4701 (1991).
- [3] L. G. Baxandall, Dynamics of reversibly crosslinked chains, *Macromolecules* **22**, 1982 (1989).
- [4] M. Rubinstein and A. N. Semenov, Thermoreversible gelation in solutions of associating polymers. 2. Linear dynamics, *Macromolecules* **31**, 1386 (1998).
- [5] M. E. Cates, Reptation of living polymers: Dynamics of entangled polymers in the presence of reversible chain-scission reactions, *Macromolecules* **20**, 2289 (1987).
- [6] M. Rubinstein and A. N. Semenov, Dynamics of entangled solutions of associating polymers, *Macromolecules* **34**, 1058 (2001).
- [7] A. N. Semenov and M. Rubinstein, Dynamics of entangled associating polymers with large aggregates, *Macromolecules* **35**, 4821 (2002).
- [8] A. N. Semenov, J. F. Joanny, and A. R. Khokhlov, Associating polymers: Equilibrium and linear viscoelasticity, *Macromolecules* **28**, 1066 (1995).
- [9] F. Tanaka and S. F. Edwards, Viscoelastic properties of physically cross-linked networks. 1. Transient network theory, *Macromolecules* **25**, 1516 (1992).
- [10] M. J. Webber and M. W. Tibbitt, Dynamic and reconfigurable materials from reversible network interactions, *Nat. Rev. Mater.* **7**, 541 (2022).
- [11] M.-H. Wei, B. Li, R. L. A. David, S. C. Jones, V. Sarohia, J. A. Schmitgal, and J. A. Kornfield, Mega-supramolecules for safer, cleaner fuel by end-association of long telechelic polymers, *Science* **350**, 72 (2015).
- [12] T. J. Murdoch, E. Pashkovski, R. Patterson, R. W. Carpick, and D. Lee, Sticky but slick: Reducing friction using associative and nonassociative polymer lubricant additives, *ACS Appl. Polym. Mater.* **2**, 4062 (2020).
- [13] A. J. Reuvers, Control of rheology of water-borne paints using associative thickeners, *Prog. Org. Coat.* **35**, 171 (1999).
- [14] S. C. Grindy, R. Learsch, D. Mozhdehi, J. Cheng, D. G. Barrett, Z. Guan, P. B. Messersmith, and N. Holten-Andersen, Control of hierarchical polymer mechanics with bioinspired metal-coordination dynamics, *Nat. Mater.* **14**, 1210 (2015).
- [15] E. Filippidi, T. R. Cristiani, C. D. Eisenbach, J. Herbert Waite, J. N. Israelachvili, B. Kollbe Ahn, M. T. Valentine, J. H. Waite, J. N. Israelachvili, B. Kollbe Ahn, and M. T. Valentine, Toughening elastomers using mussel-inspired iron-catechol complexes, *Science* **358**, 502 (2017).
- [16] B. J. B. Folmer, R. P. Sijbesma, R. M. Versteegen, J. a J. Van Der Rijt, and E. W. Meijer, Supramolecular polymer materials: Chain extension of telechelic polymers using a reactive hydrogen-bonding synthon, *Adv. Mater.* **12**, 874 (2000).
- [17] G. R. Gossweiler, G. B. Hewage, G. Soriano, Q. Wang, G. W. Welshofer, X. Zhao, and S. L. Craig, Mechanochemical activation of covalent bonds in polymers with full and repeatable macroscopic shape recovery, *ACS Macro Lett.* **3**, 216 (2014).
- [18] P. Cordier, F. Tournilhac, C. Soulié-Ziakovic, L. Leibler, C. Soulie-Ziakovic, and L. Leibler, Self-healing and thermoreversible rubber from supramolecular assembly, *Nature (London)* **451**, 977 (2008).
- [19] Y. L. Chen, A. M. Kushner, G. A. Williams, and Z. B. Guan, Multiphase design of autonomic self-healing thermoplastic elastomers, *Nat. Chem.* **4**, 467 (2012).
- [20] M. Burnworth, L. Tang, J. R. Kumpfer, A. J. Duncan, F. L. Beyer, G. L. Fiore, S. J. Rowan, and C. Weder, Optically healable supramolecular polymers, *Nature (London)* **472**, 334 (2011).
- [21] M. J. Webber, E. A. Appel, E. W. Meijer, and R. Langer, Supramolecular biomaterials, *Nat. Mater.* **15**, 13 (2015).
- [22] A. M. Rosales and K. S. Anseth, The design of reversible hydrogels to capture extracellular matrix dynamics, *Nat. Rev. Mater.* **1**, 1 (2016).
- [23] Z. Zhang, C. Huang, R. A. Weiss, and Q. Chen, Association energy in strongly associative polymers, *J. Rheol.* **61**, 1199 (2017).
- [24] D. Amin, A. E. Likhtman, and Z. Wang, Dynamics in supramolecular polymer networks formed by associating telechelic chains, *Macromolecules* **49**, 7510 (2016).
- [25] E. B. Stukalin, L.-H. Cai, N. A. Kumar, L. Leibler, and M. Rubinstein, Self-healing of unentangled polymer networks with reversible bonds, *Macromolecules* **46**, 7525 (2013).
- [26] R. S. Hoy and G. H. Fredrickson, Thermoreversible associating polymer networks. I. Interplay of thermodynamics, chemical kinetics, and polymer physics, *J. Chem. Phys.* **131**, 1 (2009).
- [27] A. Ghosh and K. S. Schweizer, Physical bond breaking in associating copolymer liquids, *ACS Macro Lett.* **10**, 122 (2021).
- [28] A. Ghosh, S. Samanta, S. Ge, A. P. Sokolov, and K. S. Schweizer, Influence of attractive functional groups on the segmental dynamics and glass transition in associating polymers, *Macromolecules* **55**, 2345 (2022).
- [29] A. Ghosh and K. S. Schweizer, Microscopic theory of the effect of caging and physical bonding on segmental relaxation in associating copolymer liquids, *Macromolecules* **53**, 4366 (2020).
- [30] Q. Chen, G. J. Tudryn, and R. H. Colby, Ionomer dynamics and the sticky Rouse model, *J. Rheol.* **57**, 1441 (2013).
- [31] A. Mordvinkin, D. Döhler, W. H. Binder, R. H. Colby, and K. Saalwächter, Terminal Flow of Cluster-Forming Supramolecular Polymer Networks: Single-Chain Relaxation or Micelle Reorganization?, *Phys. Rev. Lett.* **125**, 127801 (2020).
- [32] S. Tang, M. Wang, and B. D. Olsen, Anomalous self-diffusion and sticky Rouse dynamics in associative protein hydrogels, *J. Am. Chem. Soc.* **137**, 3946 (2015).

- [33] T. Yan, K. Schröter, F. Herbst, W. H. Binder, and T. Thurn-Albrecht, Nanostructure and rheology of hydrogen-bonding telechelic polymers in the melt: From micellar liquids and solids to supramolecular gels, *Macromolecules* **47**, 2122 (2014).
- [34] K. Xing, M. Tress, P. Cao, S. Cheng, T. Saito, V. N. Novikov, and A. P. Sokolov, Hydrogen-bond strength changes network dynamics in associating telechelic PDMS, *Soft Matter* **14**, 1235 (2018).
- [35] S. Ge, S. Samanta, B. Li, G. P. Carden, P. F. Cao, and A. P. Sokolov, Unravelling the mechanism of viscoelasticity in polymers with phase-separated dynamic bonds, *ACS Nano* **16**, 4746 (2022).
- [36] S. Ge, S. Samanta, M. Tress, B. Li, K. Xing, P. Dieudonné-George, A. C. Genix, P. F. Cao, M. Dadmun, and A. P. Sokolov, Critical role of the interfacial layer in associating polymers with microphase separation, *Macromolecules* **54**, 4246 (2021).
- [37] S. Ge, M. Tress, K. Xing, P. F. Cao, T. Saito, and A. P. Sokolov, Viscoelasticity in associating oligomers and polymers: Experimental test of the bond lifetime renormalization model, *Soft Matter* **16**, 390 (2020).
- [38] D. J. M. Van Beek, A. J. H. Spiering, G. W. M. Peters, K. Te Nijenhuis, and R. P. Sijbesma, Unidirectional dimerization and stacking of ureidopyrimidinone end groups in polycaprolactone supramolecular polymers, *Macromolecules* **40**, 8464 (2007).
- [39] J. Wu, L.-H. Cai, and D. A. D. A. Weitz, Tough self-healing elastomers by molecular enforced integration of covalent and reversible networks, *Adv. Mater.* **29**, 1702616 (2017).
- [40] See Supplemental Material at <http://link.aps.org/supplemental/10.1103/PhysRevLett.130.228101> for polymer synthesis and characterization, materials and methods, simulation details, and additional discussions, which includes Refs. [41–56].
- [41] J. E. Mark, *Physical Properties of Polymers Handbook*, 2nd ed. (Springer Science & Business Media, New York, 2007).
- [42] T. A. Kavassalis and J. Noolandi, New View of Entanglements in Dense Polymer Systems, *Phys. Rev. Lett.* **59**, 2674 (1987).
- [43] K. Matyjaszewski, W. Jakubowski, K. Min, W. Tang, J. Huang, W. A. Braunecker, and N. V. Tsarevsky, Diminishing catalyst concentration in atom transfer radical polymerization with reducing agents, *Proc. Natl. Acad. Sci. U.S.A.* **103**, 15309 (2006).
- [44] S. Nian, H. Lian, Z. Gong, M. Zhernenkov, J. Qin, and L.-H. Cai, Molecular architecture directs linear-bottlebrush-linear triblock copolymers to self-assemble to soft reprocessable elastomers, *ACS Macro Lett.* **8**, 1528 (2019).
- [45] S. Nian, J. Zhu, H. Zhang, Z. Gong, G. Freychet, M. Zhernenkov, B. Xu, and L. H. Cai, Three-dimensional printable, extremely soft, stretchable, and reversible elastomers from molecular architecture-directed assembly, *Chem. Mater.* **33**, 2436 (2021).
- [46] S. Nian, B. Huang, G. Freychet, M. Zhernenkov, and L.-H. Cai, Unexpected folding of bottlebrush polymers in melts, *Macromolecules* **56**, 2551 (2023).
- [47] M. Zhernenkov, N. Canestrari, O. Chubar, and E. DiMasi, Soft matter interfaces beamline at NSLS-II: Geometrical ray-tracing vs. wavefront propagation simulations, in *Advances in Computational Methods for X-Ray Optics III*, edited by M. Sanchez del Rio and O. Chubar (International Society for Optics and Photonics, San Diego, California, 2014), Vol. 9209, p. 92090G, [10.1117/12.2060889](https://doi.org/10.1117/12.2060889).
- [48] R. J. Pandolfi *et al.*, Xi-Cam: A versatile interface for data visualization and analysis, *J. Synchrotron Radiat.* **25**, 1261 (2018).
- [49] C. Liu, J. He, E. van Ruymbeke, R. Keunings, and C. Bailly, Evaluation of different methods for the determination of the plateau modulus and the entanglement molecular weight, *Polymer* **47**, 4461 (2006).
- [50] A. Afantitis, G. Melagraki, K. Makridima, A. Alexandridis, H. Sarimveis, and O. Iglessi-Markopoulou, Prediction of high weight polymers glass transition temperature using RBF neural networks, *J. Mol. Struct. Theochem.* **716**, 193 (2005).
- [51] P. C. Hiemenz and T. P. Lodge, *Polymer Chemistry*, 2nd ed. (CRC Press, Boca Raton, 2007).
- [52] M. L. Williams, R. F. Landel, and J. D. Ferry, The temperature dependence of relaxation mechanisms in amorphous polymers and other glass-forming liquids, *J. Am. Chem. Soc.* **77**, 3701 (1955).
- [53] W. L. Jorgensen, D. S. Maxwell, and J. Tirado-Rives, Development and testing of the OPLS all-atom force field on conformational energetics and properties of organic liquids, *J. Am. Chem. Soc.* **118**, 11225 (1996).
- [54] A. I. Jewett, D. Stelter, J. Lambert, S. M. Saladi, O. M. Roscioni, M. Ricci, L. Autin, M. Maritan, S. M. Bashusqeh, T. Keyes, R. T. Dame, J. E. Shea, G. J. Jensen, and D. S. Goodsell, Moltemplate: A tool for coarse-grained modeling of complex biological matter and soft condensed matter physics, *J. Mol. Biol.* **433**, 166841 (2021).
- [55] A. P. Thompson, H. M. Aktulga, R. Berger, D. S. Bolintineanu, W. M. Brown, P. S. Crozier, P. J. in 't Veld, A. Kohlmeyer, S. G. Moore, T. D. Nguyen, R. Shan, M. J. Stevens, J. Tranchida, C. Trott, and S. J. Plimpton, LAMMPS—a flexible simulation tool for particle-based materials modeling at the atomic, meso, and continuum scales, *Comput. Phys. Commun.* **271**, 108171 (2022).
- [56] H. E. Gottlieb, V. Kotlyar, and A. Nudelman, NMR chemical shifts of common laboratory solvents as trace impurities, *J. Org. Chem.* **62**, 7512 (1997).
- [57] S. Nian, Z. Fan, G. Freychet, M. Zhernenkov, S. Redemann, and L. H. Cai, Self-assembly of flexible linear-semiflexible bottlebrush-flexible linear triblock copolymers, *Macromolecules* **54**, 9361 (2021).
- [58] A. J. Doig and D. H. Williams, Binding-energy of an amide-amide hydrogen bond in aqueous and nonpolar solvents, *J. Am. Chem. Soc.* **114**, 338 (1992).
- [59] P. Bonardelli, G. Moggi, and A. Turturro, Glass transition temperatures of copolymer and terpolymer fluoroelastomers, *Polymer* **27**, 905 (1986).
- [60] M. Rubinstein and R. H. Colby, *Polymer Physics* (Oxford University Press, Oxford, UK, 2003).
- [61] R. Böhmer, K. L. Ngai, C. A. Angell, and D. J. Plazek, Nonexponential relaxations in strong and fragile glass formers, *J. Chem. Phys.* **99**, 4201 (1993).
- [62] T. Yan, K. Schröter, F. Herbst, W. H. Binder, and T. Thurn-Albrecht, What controls the structure and the linear

- and nonlinear rheological properties of dense, dynamic supramolecular polymer networks?, *Macromolecules* **50**, 2973 (2017).
- [63] S. Wu and Q. Chen, Advances and new opportunities in the rheology of physically and chemically reversible polymers, *Macromolecules* **55**, 697 (2022).
- [64] X. Cao, X. Yu, J. Qin, and Q. Chen, Reversible gelation of entangled ionomers, *Macromolecules* **52**, 8771 (2019).
- [65] Q. Chen, C. Huang, R. A. Weiss, and R. H. Colby, Viscoelasticity of reversible gelation for ionomers, *Macromolecules* **48**, 1221 (2015).
- [66] B. Mei, Y. Zhou, and K. S. Schweizer, Experimental test of a predicted dynamics-structure-thermodynamics connection in molecularly complex glass-forming liquids, *Proc. Natl. Acad. Sci. U.S.A.* **118**, 1 (2021).